ELSEVIER

Journal of Chromatography A, 908 (2001) 215–221

JOURNAL OF CHROMATOGRAPHY A

www.elsevier.com/locate/chroma

Calculation of partition coefficient and hydrophobic moment of the secondary structure of lysozyme

Francisco Torrens*

Departament de Quimíca Física, Facultat de Química, Universitat de València, Dr. Moliner 50, E-46 100 Burjassot, València, Spain

Abstract

A method that permits a semiquantitative estimate of the partitioning of any solute between any two media is presented. As an example, the partition coefficients and hydrophobic moment of the secondary structure of lysozyme are calculated. Program GSCAP is written as a version of Pascal's solvent-dependent conformational analysis (SCAP) program. The dipole moments calculated for the helices are trebled with respect to that for the sheet. For helices, the main contribution to the water-accessible surface area is the hydrophobic term, while the hydrophilic part dominates in the sheet. Molecular globularity and the three studied partition coefficients differentiate between helices and sheet.

Keywords: Partition coefficients; Hydrophobicity; Solvation parameter model; Thermodynamic parameters; Lysozyme; Proteins

1. Introduction

Free energy is the fundamental thermodynamic variable controlling equilibria, and free energy of solvation is the free-energy difference between a molecule in the gas phase and in a solvent [1]. The free energy of solvation of a solute *X* in solvent *Y* may be used to predict its vapour pressure over a dilute solution (Henry's law), and the free energy of solvation of *X* in *X* may be used to predict the vapour pressure of a pure liquid or of the solvent of a dilute solution (Raoult's law) [2].

Free energy of solvation may be considered as a special case of free energy of transfer in which one of the transfer media is an inert gas, usually called *air*, and the other is a liquid. By combining the free energy of transfer of solute *X* from air into solvent *Y* with the free energy of transfer of *X* from air into solvent *Z*, one can obtain the free energy of transfer of *X* from *Y* to *Z*, which allows one to calculate partition coefficients, i.e. the equilibrium distribution of a solute between immiscible liquid media, which are of critical importance in pharmaceutical [3] and environmental [4] applications or for extractions. Comparing the free energies of solvation of conformational or tautomeric isomers X_{I} and X_{II} of molecule *X* in various solvents allows one to predict solvent effects on conformational or tautomeric equilibria [5].

Motivated by its widespread use as a bioavailability parameter in the drug industry, the partition coefficient for 1-octanol and water has received by far the most attention [6], although Abraham, for example, has developed much broader relationships applicable to almost any solvent.

While much work has been done by many groups in developing models for water, as reviewed else-

*Tel.: +34-96-398-3182; fax: +34-96-398-3156.

E-mail address: francisco.torrens@uv.es (F. Torrens).

0021-9673/01/$ – see front matter
PII: S0021-9673(00)00727-5

where [7–9], much less effort has been devoted to developing models for non-aqueous solvents [10–16]. However, a large body of data is available for 1-octanol [17] and *n*-hexadecane [18,19]. A significant amount of data is also available for other alkanes, cyclohexane, benzene, toluene, xylenes, diethyl ether, chloroform, carbon tetrachloride and chlorobenzene [20]. If one takes data from *all* organic solvents, a very large number of data are available. In this article, it is shown that it is possible to analyze these data as a whole and develop a model that encompasses a large number of solvents in a single framework.

Solvation energies for both aqueous [21] and non-aqueous solvents can be used to predict partition coefficients of solutes between an organic phase and water [22], and such partition coefficients are often used to provide some indication of how likely it is for the solute to penetrate a lipid bilayer, skin, brain, central nervous system or other biophase or to bind to a non-polar site in or on a protein [23].

Fleming discovered lysozyme (EC 3.2.1.17, mucopeptide *N*-acetylmuramylhydrolase) in 1922. In the early stages, it was studied by bacteriologists because of its lytic activity against bacteria. However, following the successful crystallization of lysozyme from hen egg-white by Abraham and Robinson in 1937 [24], the enzyme began to attract the keen attention of protein chemists. There was considerable difficulty attached to studying the structure–function relationship of lysozyme, due to the obscurity of its enzymatic activity. In 1957, Berger and Weiser [25] observed the β-*N*-acetylglucosaminidase activity of lysozyme. Moreover, soluble oligosaccharide substrates were prepared from a hydrolyzate of bacterial cell walls by Salton and Ghuysen [26]. In 1963, Jolles et al. [27] in France and Canfield [28] in the USA independently determined the amino acid sequence of hen egg-white lysozyme; the first report of its X-ray crystallographic analysis, by the Phillips group in England, appeared in 1965. More detailed information on the three-dimensional conformation of the molecule and on the substrate binding mode followed in 1967 from the work of Blake et al. [29,30]. Lysozyme is the first enzyme in which it is possible to understand the enzymatic activity on the basis of the three-dimensional fine structure of the enzyme molecule. Moreover, much progress has been made in physicochemical and enzymatic studies of lysozyme in solution [31].

The present model is an extension of the solvent-dependent conformational analysis (SCAP) 1-octanol–water model [32,33] to organic solvents, and it uses extended versions of the functional forms developed in that work [34]. The method has been previously applied to the calculation of some organic solvent–water partition coefficients of porphyrins, phthalocyanines, benzobisthiazoles, fullerenes [34], acetanilides, barbiturates and local anaesthetics [35]. In this work, the solubility in water and in a set of organic liquids, the organic solvent–water partition coefficients and the hydrophobic moment of the secondary structure regions of the lysozyme molecule have been calculated. Section 2 presents the improvements in the solvation model from Refs. [34,35]. In Section 3, the results and discussion are presented. Section 4 summarizes my conclusions.

2. Partitioning of any solute between any two media

The basis for building a method that permits a semiquantitative estimate of the partitioning of any solute between any two media has been reported elsewhere [34,35] (see illustration in Ref. [33]). The method is based on the model of Hopfinger [36,37]. The main improvement introduced with respect to Ref. [34] is the change in the standard Gibbs free energy parameter Δg_s^o calculated using the generalized Born equation [38]:

$$\Delta g_s^o = \Delta g_o^o \cdot \frac{1-(1/\varepsilon_s)}{1-(1/\varepsilon_o)} = \Delta g_o^o \cdot \frac{\varepsilon_o(\varepsilon_s-1)}{\varepsilon_s(\varepsilon_o-1)} \qquad (1)$$

where the subscripts o and s stand for 1-octanol and for a general organic solvent, respectively, and ε_o and ε_s are the relative dielectric constants [35].

The only parameters required are the Cartesian components of the solute molecule and the relative dielectric constant ε and molecular volume V_s of the organic solvent. The V_s values have been calculated with a new version of the program TOPO [33,39], which includes an actualized database of van der Waals radii [40]. In the present work, the following

values have been used: $\varepsilon = 10.34$ (1-octanol), 2.023 (cyclohexane) and 4.806 (chloroform); $V_s = 155.0$ (1-octanol), 93.4 (cyclohexane) and 72.1 (chloroform) [35].

The algorithm of Kyte and Doolittle [41] was used to calculate the hydropathy profile of the structures. The hydrophobicity of each structure is calculated from its atomic contributions as

$$H = \sum_{i=1}^{M} h_i$$

where h_i is the hydrophobicity of atom i and the sum extends to the number of atoms in the structure, M.

The hydrophobic moment calculation is based on the Eisenberg et al. formula [42–44]:

$$\mu = \left[\left(\sum_{i=1}^{M} h_i \cos \delta_i \right)^2 + \left(\sum_{i=1}^{M} h_i \sin \delta_i \right)^2 \right]^{1/2}$$

where the gyration angle δ_i is the successive angle between an atom and the next, around the z-axis. For instance, δ increases 97° in the successive C^{α} atoms of an α-helical structure. This hydrophobic moment is a widely used method for determining amphipathic helices in a protein [45,46].

3. Results and discussion

The structure of hen egg-white lysozyme was determined by the Phillips group (see illustration in Ref. [47]). The regions of helix and sheet are summarized in Table 1 and Fig. 1. As shown in the table, the parameters for the helical regions 5–15, 24–34 and 88–96 are close to those of an α-helix [31]. However, some distortion is observed, which gives an intermediate conformation between α-helix and 3.0_{10}-helix. The short helix 80–85 is very close to a 3.0_{10}-helix, while in the region 119–122 there is only a one-turn 3.0_{10}-helix. The lysozyme molecule contains an antiparallel β-structure in the region 41–54. A disulphide linkage between Cys-6 and Cys-127 joins both extremes.

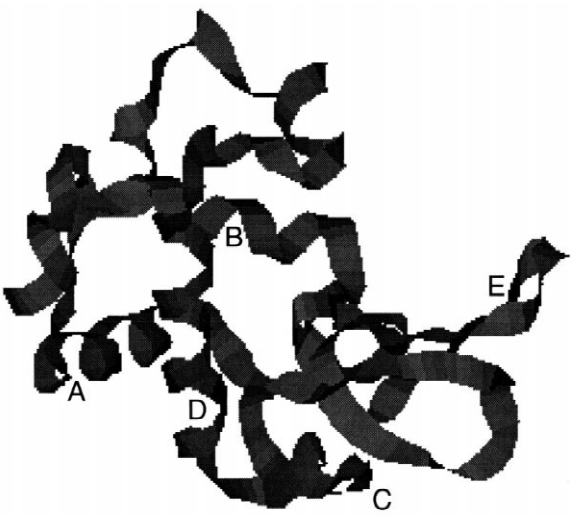

Fig. 1. Molecular image of lysozyme showing the secondary structure regions.

The molecular dipole μ and quadrupole Θ moments of the secondary structure regions in lysozyme are reported in Table 2. The calculation was performed using X-ray coordinates of the atoms of lysozyme (2LYM) [48] from the Protein Data Bank. Each structure is brought into its principal inertial coordinate system. The length x of the structure is

Table 1
Parameters of secondary structure regions in lysozyme

Structure	Region	Type	Residue	Number	Percentage
Helix	A	α	5–15	11	8.5
	B	α	24–34	11	8.5
	C	3.0_{10}	80–85	6	5
	D	α	88–96	9	7
Total helix				37	29
β-Sheet	E	Antiparallel	41–54	14	11
Total helix + sheet				51	40
Total				129	100

Table 2
Electrostatic properties for the secondary structure regions in lysozyme

Structure	μ[a] PM3	μ POLAR	Θ[b] POLAR	Θ_1[c] POLAR	Θ_2 POLAR	Θ_3 POLAR
All atoms						
A	–[d]	8.363	−73.584	64.934	18.396	−304.081
B	–[d]	6.451	33.539	69.423	38.737	−7.542
C	17.888	3.933	16.809	39.322	29.694	−18.587
D	–[d]	4.279	12.817	62.018	15.790	−39.356
Mean A–D	17.888	5.757	−2.605	58.924	25.654	−92.392
E	–[d]	3.919	43.508	156.965	44.757	−71.197
Main chain saturated with H						
A	41.048					
B	41.378					
C	17.568					
D	33.114					
Mean A–D	33.277					
E	11.169					

[a] Dipole moment (Debye).
[b] Mean quadrupole moment (D·Å).
[c] Quadrupole moment tensor eigenvalues Θ_1, Θ_2 and Θ_3 (D·Å).
[d] Maximum number of atoms exceeded.

defined as the maximal length, the height z as its minimal thickness, and its width y is measured at right angles to the x- and z-axes. The origin is taken at the centre of mass for each structure. When all the atoms are considered, the lysozyme segments are, in general, too big to be calculated with the MOPAC-PM3 method [49]. In order to overcome this difficulty, the side-chain groups have been eliminated and the main-chain atoms have been saturated with H atoms. The dipole moments μ calculated for the four A–D helices are trebled with respect to that for the E β-sheet. It should be noted that the C helix is small enough to be calculated with PM3 all-atoms (17.888 D), and the main-chain result (17.568 D) shows good agreement, with an error of −1.8%. It is assumed that this error holds for the remaining structures and the main-chain model was applied. The results obtained with POLAR [50–56] for the all-atom structures show again that $\mu_{A-D} > \mu_E$, with differences of ca. 47%. Both types of structures can also be differentiated by the mean quadrupole moment, $\Theta_{A-D} < \Theta_E$.

The geometric descriptors for the secondary structure regions in lysozyme are listed in Table 3. The descriptors have been calculated with the TOPO program [33,39]. Reference calculations have been carried out with the GEPOL program [57]. There is good agreement between both methods. For instance, errors are ca. 0.8% for the molecular volume and ca. 7% for the molecular surface area. In particular, discussion of the volumes and surfaces of the different regions is difficult because they increase with size. However, an important remark can be made. For segments in a helix, the main contribution to the water-accessible surface area is the hydrophobic HBAS term, while the hydrophilic HLAS component part dominates in the β-sheet. Thus, for the A–D helices HBAS>HLAS, with a difference of ca. 78%. On the other hand, for the E β-sheet HLAS>HBAS by 44%.

The topological indices for the secondary structure regions in lysozyme are summarized in Table 4. The molecular globularity G is greater for the A–D helices than for the E β-sheet (ca. 17%). However, the molecular rugosity G' cannot differentiate properly between both types of structures. The fractal dimension of the solvent-accessible surface D is smaller for A–D than for E (ca. 3%). Moreover, the fractal dimension averaged for non-buried atoms D' is also smaller for A–D than for E (ca. 4%).

The free energy of solvation, partition coefficient and hydrophobic moment results for the secondary structure regions in lysozyme are reported in Table 5. Minus Gibbs free energy of solvation in water is

Table 3
Geometric descriptions for the secondary structure regions in lysozyme

Structure	V (Å^3)[a]	V ref.[b]	S (Å^2)[c]	S ref.[b]	AS (Å^2)[d]	AS ref.[b]	HBAS[e]	HLAS[f]	AS′(Å^2)[g]	AS′ ref.[b]
A	1123.9	1132.5	1228.36	1316.60	1404.5	1449.3	830.6	573.9	2076.3	2103.7
B	1058.5	1068.7	1126.70	1214.69	1256.4	1295.4	863.0	393.4	1878.5	1904.2
C	517.2	520.9	582.03	618.30	767.3	788.7	502.2	265.1	1257.7	1273.6
D	807.7	815.8	876.51	944.33	978.1	1007.2	597.1	381.0	1530.8	1549.9
Mean										
A–D	876.8	884.5	953.40	1023.48	1101.6	1135.2	698.2	403.4	1685.8	1707.9
E	1259.8	1269.9	1394.89	1488.93	1438.6	1482.6	590.5	848.1	2112.0	2138.4

[a] Molecular volume (Å^3).
[b] Reference: calculations carried out with the GEPOL program.
[c] Molecular surface area (Å^2).
[d] Water-accessible surface area (Å^2).
[e] Hydrophobic-accessible surface area (Å^2).
[f] Hydrophilic-accessible surface area (Å^2).
[g] Side-chain-accessible surface area (Å^2).

Table 4
Topological indices for the secondary structure regions in lysozyme

Structure	G[a]	G ref.[b]	G'[c]	G' ref.[b]	D[d]	D ref.[b]	D'[e]
A	0.426	0.399	1.093	1.163	1.623	1.640	1.813
B	0.446	0.416	1.064	1.137	1.611	1.627	1.805
C	0.535	0.506	1.126	1.187	1.523	1.537	1.628
D	0.479	0.447	1.085	1.158	1.566	1.583	1.749
Mean							
A–D	0.472	0.442	1.092	1.161	1.581	1.597	1.749
E	0.404	0.381	1.107	1.173	1.629	1.646	1.821

[a] Molecular globularity.
[b] Reference: calculations carried out with the GEPOL program.
[c] Molecular rugosity (Å^{-1}).
[d] Fractal dimension of the solvent-accessible surface.
[e] Fractal dimension of the solvent-accessible surface average for non-buried atoms.

Table 5
Free energy of solvation, partition coefficient and hydrophobic moment results for the secondary structure regions in lysozyme

Structure	$\Delta G_{solv\ w}$[a]	$\Delta G_{solv\ o}$[b]	$\Delta G_{solv\ ch}$[c]	$\Delta G_{solv\ cf}$[d]	Log P_o[e]	Log P_{ch}[f]	Log P_{cf}[g]	μ_H[h]
A	−170.1	−244.1	−139.3	−223.0	13.0	−5.40	9.31	4.51
B	−161.3	−234.4	−134.5	−215.8	12.8	−4.70	9.58	2.71
C	−89.16	−124.9	−72.74	−117.4	6.27	−2.89	4.95	3.96
D	−133.7	−181.1	−104.6	−168.8	8.32	−5.12	6.16	5.21
Mean								
A–D	−138.6	−196.1	−112.8	−181.3	10.1	−4.53	7.50	4.10
E	−354.7	−299.7	−170.5	−272.0	−9.66	−32.4	−14.5	4.93

[a] Gibbs free energy of solvation in water (kJ mol^{-1}).
[b] Gibbs free energy of solvation in 1-octanol (kJ mol^{-1}).
[c] Gibbs free energy of solvation in cyclohexane (kJ mol^{-1}).
[d] Gibbs free energy of solvation in chloroform (kJ mol^{-1}).
[e] P_o is the 1-octanol–water partition coefficient.
[f] P_{ch} is the cyclohexane–water partition coefficient.
[g] P_{cf} is the chloroform–water partition coefficient.
[h] μ_H is the hydrophobic moment.

smaller for the A–D helices than for the E β-sheet. However, this trend is damped in the three organic solvents (1-octanol, o; cyclohexane, ch; and chloroform, cf). Therefore, the three organic solvent–water partition coefficients log P are much greater for A–D than for E. The greater values of the three log P results for A–D are related to the large HBAS in Table 3, and the lower value of the three log P results for E is related to the large HBAS (Table 3). The differences in the three P results are ca. 20 log units (P_o), 28 log units (P_{ch}) and 22 log units (P_{cf}). It should be noted that for values of $\log P > 3$, more than 99.9% of the solute is in the organic phase, and for values of $\log P < -3$, more than 99.9% of the solute is in the aqueous phase. Therefore, some results predict a negligible quantity of solute in one or the other phase. Some minus log P values are greater than the Avogadro number exponent 23 ($P < 10^{-23}$). This would mean that no solute molecules would be present in the organic phase to allow experiments for validation. However, all log P figures are reported in Table 5 for the purpose of comparison along the series of secondary structure regions.

On the other hand, the hydrophobic moment μ_H cannot differentiate properly between both types of secondary structures.

4. Conclusions

A method that permits a semiquantitative estimate of the partitioning of any solute between any two media is presented. The model is based on the modification of a previously established model known as SCAP and proposed by Hopfinger [36,37]. The hallmark of the model is that it has been designed for *all* organic solvents without previous fitting parametrization. It is based on the division of ΔG^{o}_{solv} in order to obtain a system of increments by atoms or by groups. As an example, the organic solvent–water partition coefficient P and hydrophobic moment μ_H of the secondary structure of lysozyme have been calculated. The secondary structure of lysozyme consists of four helices and one sheet. From the preceding results the following conclusions can be drawn.

1. The dipole moments calculated for the helices are trebled with respect to that for the sheet. However, the mean quadrupole moment is calculated greater for the sheet.
2. For segments in a helix, the main contribution to the water-accessible surface area is the hydrophobic term, while the hydrophilic component part dominates in the β-sheet. This is related to the greater value of the three organic solvent–water partition coefficients for the helices than for the sheet.
3. Helices and sheet have been differentiated by some topological indices, especially by the molecular globularity.
4. The program GSCAP has been written as a version of Pascal's SCAP program implementing the modelling of the solubility in any organic solvent and the calculations of organic solvent–water log *P*. The only parameters required are the dielectric constant and molecular volume of the organic solvent of interest. No fitted parameters are included in the model.
5. The three studied organic solvent–water partition coefficients differentiate between helices and sheet. The difference in log P is ca. 23 log units.

Acknowledgements

The author acknowledges financial support from the Dirección General de Enseñanza Superior of the Spanish MEC (project PB97-1383).

References

[1] A. Ben-Naim, Solvation Thermodynamics, Plenum, New York, 1987.
[2] I.M. Klotz, R.M. Rosenberg, Chemical Thermodynamics, Benjamin/Cummings, Menlo Park, CA, 1986.
[3] R.B. Silverman, The Organic Chemistry of Drug Design and Drug Action, Academic Press, San Diego, CA, 1992.
[4] R.A. Larson, E.J. Weber, Reaction Mechanisms in Environmental Organic Chemistry, Lewis, Boca Raton, FL, 1994.
[5] C. Reichardt, Solvents and Solvent Effects in Organic Chemistry, VCH, New York, 1990.
[6] C. Hansch, A. Leo, Exploring QSAR — Fundementals and Applications in Chemistry and Biology, American Chemical Society, Washington, DC, 1995.
[7] B. Honig, K. Sharp, A.-S. Yang, J. Phys. Chem. 97 (1993) 1101.

[8] J. Tomasi, M. Persico, Chem. Rev. 94 (1994) 2027.
[9] C.J. Cramer, D.G. Truhlar (Eds.), Structure and Reactivity in Aqueous Solution, American Chemical Society, Washington, DC, 1994.
[10] R. Bonaccorsi, F. Floris, J. Tomasi, J. Mol. Liq. 47 (1990) 25.
[11] R. Bonaccorsi, F. Floris, P. Palla, J. Tomasi, Therrnochim. Acta 162 (1990) 213.
[12] D.J. Giesen, J.W. Storer, C.J. Cramer, D.G. Truhlar, J. Am. Chem. Soc. 117 (1995) 1057.
[13] D.J. Giesen, C.J. Cramer, D.G. Truhlar, J. Phys. Chem. 99 (1995) 7137.
[14] D. Sitkoff, N. Ben-Tal, B. Honig, J. Phys. Chem. 100 (1996) 2744.
[15] F.J. Luque, Y. Zhang, C. Alemán, M. Bachs, J. Gao, M. Orozco, J. Phys. Chem. 100 (1996) 4269.
[16] F.J. Luque, C. Alemán, M. Bachs, M. Orozco, J. Comput. Chem. 17 (1996) 806.
[17] A.J. Leo, Chem. Rev. 93 (1993) 1281.
[18] M.H. Abraham, G.S. Whiting, R. Fuchs, F.J. Chambers, J. Chem. Soc., Perkins Trans. 2 (1990) 291.
[19] Y. Zhang, A.J. Dallas, P.W. Carr, J. Chromatogr. 638 (1993) 43.
[20] A.J. Leo, Masterfile database from MEDCHEM software, 1994.
[21] C.C. Chambers, G.D. Hawkins, C.J. Cramer, D.G. Truhlar, J. Phys. Chem. 100 (1996) 16385.
[22] D.J. Giesen, C.C. Chambers, C.J. Cramer, D.G. Truhlar, J. Phys. Chem. B 101 (1997) 5084.
[23] A. Leo, C. Hansch, D. Elkins, Chem. Rev. 71 (1971) 525.
[24] E.P. Abraham, R. Robinson, Nature (London) 140 (1937) 24.
[25] L.R. Berger, R.S. Weiser, Biochim. Biophys. Acta 26 (1957) 517.
[26] M.R.J. Salton, J.M. Ghuysen, Biochim. Biophys. Acta 36 (1959) 552.
[27] J. Jolles, J. Jauregui-Adell, I. Bernier, P. JolIes, Biochim. Biophys. Acta 78 (1963) 668.
[28] R.E. Canfield, J. Biol. Chem. 238 (1963) 2698.
[29] C.C.F. Blake, G.A. Mair, A.C.T. North, D.C. Phillips, V.R. Sarma, Proc. R. Soc. London B167 (1967) 365.
[30] C.C.F. Blake, L.N. Johnson, G.A. Mair, A.C.T. North, D.C. Phillips, V.R. Sarma, Proc. R. Soc. London B 167 (1967) 378.
[31] K. Hamaguchi, K. Hayashi, Lysozyme, in: M. Funatsu, K. Hiromi, K. Imahori, T. Mtirachi, K. Narita (Eds.), Proteins Structure and Function, Vol. 1, Kodansha, Tokyo, 1972, p. 85, Chapter 2.
[32] P. Pascal, Program SCAP, Université Henri Poincaré, Nancy I, 1991.
[33] F. Torrens, I. Sánchez-Marín, I. Nebot-Gil, J. Mol. Graphics Mod. 16 (1998) 57.
[34] F. Torrens, I. Sánchez-Marín, I. Nebot-Gil, J. Chromatogr. A 827 (1998) 345.
[35] F. Torrens, J. Chem. Inf. Comput. Sci. 40 (2000) 236.
[36] A.J. Hopfinger, Macromolecules 4 (1971) 731.
[37] A.J. Hopfinger, R.D. Batrershell, J. Med. Chem. 19 (1976) 569.
[38] M. Born, Z. Phys. 1 (1920) 45.
[39] F. Torrens, E. Ortí, J. Sánchez-Marín, J. Chim. Phys. Phys.-Chim. Biol. 88 (1991) 2435.
[40] D.R. Flower, J. Mol. Graphics Mod. 15 (1997) 238.
[41] J. Kyte, R.F. Doolittle, J. Mol. Biol. 157 (1982) 105.
[42] D. Eisenberg, E. Schwarz, M. Komaomy, R. Wall, J. Mol. Biol. 179 (1984) 125.
[43] D. Eisenberg, Annu. Rev. Biochem. 53 (1984) 595.
[44] D. Eisenberg, R.M. Weiss, T.C. Terwilliger, Proc. Natl. Acad. Sci. USA 81 (1984) 140.
[45] J.J. Pellequer, E. Westhof, J. Mol. Graphics 11 (1993) 204.
[46] X. Gallet, F. Festy, P. Ducarme, R. Brasseur, A. Thomas-Soumarmon, J. Mol. Graphics Mod. 16 (1998) 72.
[47] D.C. Phillips, Sci. Am. 215 (1966) 78.
[48] C.E. Kundrot, F.M. Richards, J. Mol. Biol. 193 (1987) 157.
[49] J.J.P. Stewart, J. Comput. Chem. 10 (1989) 209.
[50] F. Torrens, J. Sánchez-Marín, I. Nebot-Gil, J. Mol. Graphics 14 (1996) 245.
[51] F. Torrens, J. Mol. Catal. A 119 (1997) 393.
[52] F. Torrens, J. Sánchez-Marín, I. Nebot-Gil, J. Mol. Struct. (Theochem) 426 (1998) 105.
[53] F. Torrens, J. Sánchez-Marín, I. Nebot-Gil, J. Mol. Struct. (Theochem) 463 (1999) 27.
[54] F. Torrens, J. Sánchez-Marín, I. Nebot-Gil, Molecules 4 (1999) 28.
[55] F. Torrens, Microelectron. Eng. 51–52 (2000) 613.
[56] F. Torrens. Molecules, submitted for publication.
[57] J.L. Pascual-Ahuir, E. Silla, J. Tomasi, R. Bonaccorsi, J. Comput. Chem. 8 (1987) 778.